Solid State Ionics 66 (1993) 295–305
North-Holland

SOLID STATE IONICS

Oxygen permeation modelling of perovskites

Bart A. van Hassel, Tatsuya Kawada, Natsuko Sakai, Harumi Yokokawa, Masayuki Dokiya
National Institute of Materials and Chemical Research, Tsukuba Research Center, Ibaraki 305, Japan

and

Henny J.M. Bouwmeester
Laboratory for Inorganic Chemistry, Materials Science and Catalysis, Department of Chemical Technology, University of Twente, P.O. Box 217, 7500 AE Enschede, The Netherlands

Received 25 February 1993; accepted for publication 7 July 1993

A point defect model was used to describe the oxygen nonstoichiometry of the perovskites $La_{0.75}Sr_{0.25}CrO_3$, $La_{0.9}Sr_{0.1}FeO_3$, $La_{0.9}Sr_{0.1}CoO_3$ and $La_{0.8}Sr_{0.2}MnO_3$ as a function of the oxygen partial pressure. Form the oxygen vacancy concentration predicted by the point defect model, the ionic conductivity was calculated assuming a vacancy diffusion mechanism. The ionic conductivity was combined with the Wagner model for the oxidation of metals to yield an analytical expression for the oxygen permeation current density as a function of the oxygen partial pressure gradient. A linear boundary condition was used to show the effect of a limiting oxygen exchange rate at the surface.

1. Introduction

The $A_{1-y}A'_yBO_3$ (A=La, Y; A'=Ca, Sr; B=Cr, Fe, Co, Mn) perovskite materials have great technological applications in which oxygen diffusion affects their performance. For instance, $La_{1-y}Ca_yCrO_3$ is used as a separator or bipolar plate in a solid oxide fuel cell [1]. The diffusion of oxygen through the perovskite from the air side to the fuel side should be as small as possible as it will burn fuel without generating current [2,3]. $La_{1-y}Sr_yMnO_3$ is considered to be one of the best cathode materials in this solid oxide fuel cell [4]. The performance can be improved if it would be possible to increase the ionic conductivity.

$La_{0.35}Sr_{0.65}Co_{0.7}Fe_{0.3}O_{3-\delta}$ can be used as the active part in oxygen gas sensors [28]. The oxygen partial pressure dependence of the total conductivity determines the sensitivity of the sensor to changes in the oxygen partial pressure. The response time of the sensor is partially determined by oxygen diffusion in the perovskite.

The permeation of oxygen through the $La_{1-y}Sr_yCo_{1-x}Fe_xO_3$ perovskite drew attention by the study of Teraoka et al. [5]. With a membrane thickness of 1 mm, the oxygen permeation current density through $La_{0.6}Sr_{0.4}Co_{0.8}Fe_{0.2}O_3$ reached a value of 155 mA cm^{-2} in the small oxygen partial pressure gradient of 1 atm to 10^{-4} atm at 800°C. Those high fluxes in combination with a selectivity of 1 for oxygen make it possible to use the material as a ceramic membrane for gas separation applications. The material can also be used as a membrane in a catalytic reactor. The permeating oxygen can then be used for selective oxidation reactions [6].

The chemical diffusion of oxygen in an oxide showing both oxygen ion and electronic conductivity can be described within the framework of Wagner's theory for the oxidation of metals [7]. In this theory the fluxes of the oxygen ions and electrons or holes are related to each other by the condition of charge neutrality. So far, the application of this theory to model the oxygen permeation of the $A_{1-y}A'_yBO_3$ (A=La, Y; A'=Ca, Sr; B=Cr, Fe, Co, Mn) perovskites has been limited to a small oxygen partial pressure gradient [6,8–10] in which the ionic con-

Elsevier Science Publishers B.V.

ductivity was assumed to be constant. But even in a small oxygen partial pressure gradient of 1 atm to 10^{-4} atm, the ionic conductivity can vary over orders of magnitude.

The application of Wagner's theory to the oxygen permeation through the $La_{0.75}Sr_{0.25}CrO_3$, $La_{0.9}Sr_{0.1}FeO_3$, $La_{0.9}Sr_{0.1}CoO_3$ and $La_{0.8}Sr_{0.2}MnO_3$ perovskites in a large oxygen partial pressure gradient is pursued in this paper. In this case, the oxygen partial pressure dependence of their ionic conductivity should be known. Assuming a vacancy diffusion mechanism, the ionic conductivity can be calculated form data of oxygen nonstoichiometry [11–15] and vacancy diffusion coefficients [16,17]. This gives a new analytical expression which describes the oxygen permeation current density as a function of the oxygen partial pressure gradient.

2. Theory

2.1. Point defect model

2.1.1. Oxygen deficient perovskite

The oxygen nonstoichiometry of $La_{1-y}Sr_yCrO_3$, $La_{1-y}Sr_yFeO_3$ and $La_{1-y}Sr_yCoO_3$ can all be described with the same point defect model [11–14] when the Sr content is small. $La_{1-y}Sr_yMnO_3$ behaves slightly different. It shows, for instance, an oxygen excess at high oxygen partial pressures [15]. Therefore, a different defect model will be presented for this perovskite.

To make the model presentation more illustrative, the general chemical formula $A_{1-y}A'_yBO_3$ (A=La, Y; A'=Ca, Sr; B=Cr, Fe, Co, Mn) is replaced by $La_{1-y}Sr_yFeO_3$. The incorporation of $SrFeO_3$ in $LaFeO_3$ is electrically compensated by the formation of Fe^{4+} cations:

$$SrFeO_3 \xrightarrow[LaFeO_3]{} Sr'_{La} + Fe^{\cdot}_{Fe} + 3O^{\times}_{O}\,, \qquad (1)$$

where in Kröger–Vink notation [18], Sr'_{La} is a Sr^{2+} cation on a La^{3+} lattice position, $Fe^{\cdot}_{Fe}$ is a Fe^{4+} cation on a Fe^{3+} lattice position and $O^{\times}_{O}$ is an O^{2-} ion on a regular site in the perovskite lattice. The nonstoichiometry can be described by the following defect reaction:

$$2Fe^{\cdot}_{Fe} + O^{\times}_{O} \rightleftarrows 2Fe^{\times}_{Fe} + V^{\cdot\cdot}_{O} + \tfrac{1}{2}O_2(g)\,. \qquad (2)$$

Oxygen vacancies $V^{\cdot\cdot}_{O}$) are formed and Fe^{4+} cations are reduced to Fe^{3+} ($Fe^{\times}_{Fe}$) at low oxygen partial pressures.

It is assumed that the B site cations, Fe in this case, show charge disproportionation by:

$$2Fe^{\times}_{Fe} \rightleftarrows Fe'_{Fe} + Fe^{\cdot}_{Fe}\,. \qquad (3)$$

If the defects are assumed to be randomly distributed and non interactive, the Law of Mass Action gives the equilibrium constants K_2 and K_3 for the reactions 2 and 3, respectively:

$$K_2 = \frac{[Fe^{\times}_{Fe}]^2[V^{\cdot\cdot}_{O}]P_{O_2}^{1/2}}{[Fe^{\cdot}_{Fe}]^2[O^{\times}_{O}]}\,, \qquad (4)$$

$$K_3 = \frac{[Fe'_{Fe}][Fe^{\cdot}_{Fe}]}{[Fe^{\times}_{Fe}]^2}\,, \qquad (5)$$

where $[Sr'_{La}]$, $[Fe'_{Fe}]$, $[V^{\cdot\cdot}_{O}]$, $Fe^{\cdot}_{Fe}]$, $[Fe^{\times}_{Fe}]$ and $[O^{\times}_{O}]$ represent the mole fraction of the defects involved in the reactions (2) and (3). The charge neutrality condition can be represented by:

$$[Sr'_{La}] + [Fe'_{Fe}] = 2[V^{\cdot\cdot}_{O}] + [Fe^{\cdot}_{Fe}]\,. \qquad (6)$$

A fixed A/B site ratio is maintained when the following condition is fulfilled:

$$[Fe^{\times}_{Fe}] + [Fe'_{Fe}] + [Fe^{\cdot}_{Fe}] = 1\,. \qquad (7)$$

The equilibrium oxygen partial pressure of the per-

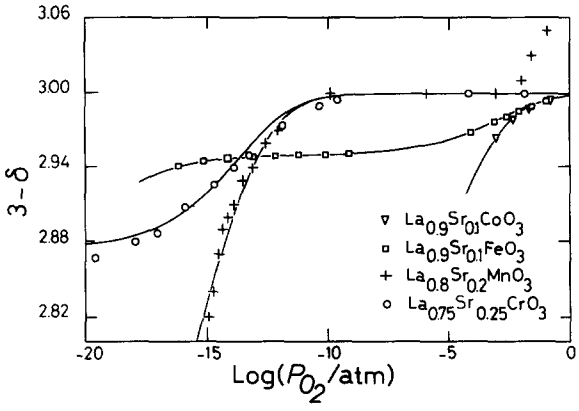

Fig. 1. A comparison between the experimentally determined refs. [11–15] (symbol) and the calculated nonstoichiometry (drawn line) of $La_{0.75}Sr_{0.25}CrO_3$, $La_{0.9}Sr_{0.1}FeO_3$, $La_{0.9}Sr_{0.1}CoO_3$ and $La_{0.8}Sr_{0.2}MnO_3$ at 1000°C using the model parameters of table 1. δ denotes the mole fraction of doubly charged oxygen vacancies ($\delta = [V^{\cdot\cdot}_{O}]$).

Table 1
Model parameters for the calculation of the nonstoichiometry and oxygen permeation at 1000°C.

Parameter	$La_{1-y}Sr_yCrO_3$	$La_{1-y}Sr_yFeO_3$	$La_{1-y}Sr_yCoO_3$	$La_{1-y}Sr_yMnO_3$
y	0.25	0.1	0.1	0.2
V_m ($m^3 mol^{-1}$) [a]	3.38×10^{-5}	3.62×10^{-5}	3.40×10^{-5}	3.56×10^{-5}
D_V ($m^2 s^{-1}$) [b]	10^{-11}	7.05×10^{-10}	9.76×10^{-10}	7×10^{-10}
K_2 ($atm^{1/2}$)	9×10^{-8}	7×10^{-2}	9×10^{-3}	4×10^{-8}
K_3	$<10^{-4}$	10^{-6}	3.5×10^{-2}	9.5×10^{-2}

[a] The molar volumes of the Sr-doped perovskites were calculated from their cell parameters as published in the Powder Diffraction File [29].

[b] The oxygen vacancy diffusion coefficients of $La_{0.9}Sr_{0.1}FeO_3$ and $La_{0.9}Sr_{0.1}CoO_3$ were taken from ref. [17]. The D_V of $La_{0.8}Sr_{0.2}MnO_3$ was calculated from the tracer diffusion coefficient of oxygen in $La_{0.65}Sr_{0.35}MnO_3$, $D^* = 3\times10^{-13}$ $cm^2 s^{-1}$ at 900°C [30], assuming an oxygen vacancy mole fraction of $[V_O^{\cdot\cdot}] = 3\times10^{-7}$ and an activation energy of 100 kJ/mol. The D_V of $La_{0.75}Sr_{0.25}CrO_3$ resulted from the oxygen permeation measurements of $La_{0.7}Ca_{0.3}CrO_3$ performed by Sakai et al. [26].

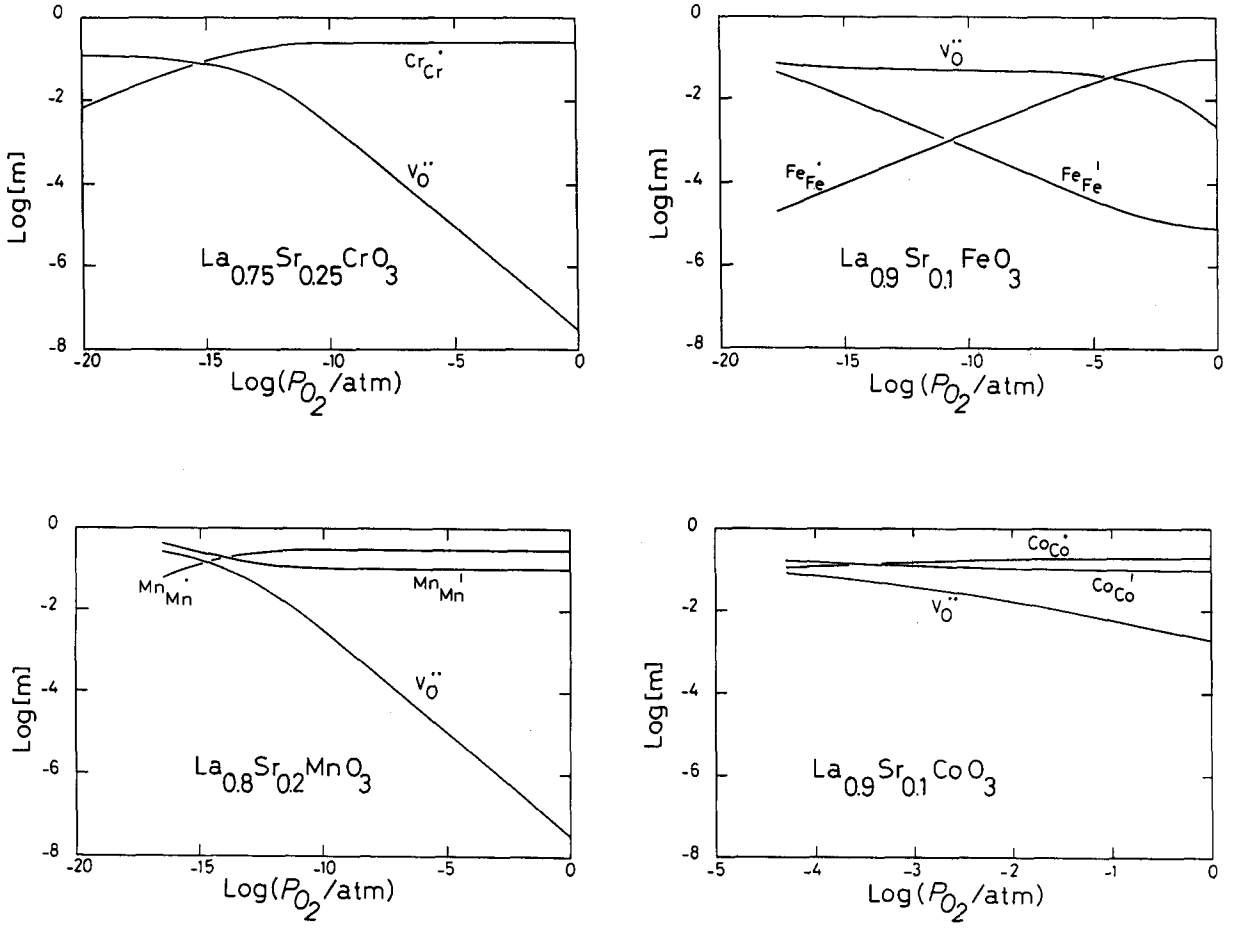

Fig. 2. Mole fraction of the defects involved in the defect reactions (2) and (3) as a function of the oxygen partial pressure for $La_{0.75}Sr_{0.25}CrO_3$, $La_{0.9}Sr_{0.1}FeO_3$, $La_{0.9}Sr_{0.1}CoO_3$ and $La_{0.8}Sr_{0.2}MnO_3$ at 1000°C, using the model parameters of table 1.

ovskite can now be calculated as a function of the mole fraction of the point defects involved in the reactions (2) and (3):

$$P_{O_2} = \left(\frac{K_2 K_3 [Fe_{Fe}^{\cdot}][O_O^{\times}]}{[Fe_{Fe}'][V_O^{\cdot\cdot}]} \right)^2 . \quad (8)$$

In fig. 1, experimental data of the nonstoichiometry of the $La_{0.75}Sr_{0.25}CrO_3$, $La_{0.9}Sr_{0.1}FeO_3$, $La_{0.9}Sr_{0.1}CoO_3$ and $La_{0.8}Sr_{0.2}MnO_3$ perovskites [11–15] are compared with the nonstoichiometry calculated from the model parameters given in table 1. Close agreements are seen between the experimentally determined and calculated nonstoichiometry for the Cr, Mn, Fe and Co-perovskites. The resulting defect mole fractions as a function of the oxygen partial pressure are shown in fig. 2.

2.1.2. *Oxygen excess perovskite*

As shown in fig. 1, the random point defect model described in Section 2.1.1 cannot explain any oxygen excess observed in $La_{1-y}Sr_yMnO_3$ at high oxygen partial pressures. The oxygen excess may result from an equal amount of A and B site vacancies by the following defect reaction [15]:

$$6Mn_{Mn}^{\times} + \tfrac{3}{2}O_2 \rightleftarrows V_{La}''' + V_{Mn}''' + 6Mn_{Mn}^{\cdot} + 3O_O^{\times} , \quad (9)$$

with the equilibrium constant:

$$K_9 = \frac{[V_{La}'''][V_{Mn}'''][Mn_{Mn}^{\cdot}]^6[O_O^{\times}]^3}{[Mn_{Mn}^{\times}]^6 P_{O_2}^{3/2}} . \quad (10)$$

If the defect reactions (2) and (3) are used together with the defect reaction (9), than a better fit can be obtained between the experimental determined nonstoichiometry of $La_{1-y}Sr_yMnO_3$ [15] and the model calculation, as shown in fig. 3a. However, the calculation of the defect mole fractions with the model parameters of table 2 ($La_{1-y}Sr_yMnO_3$ "excess") is not satisfactory as it predicts very high Mn^{2+} cation fractions even at high oxygen partial pressures, as shown in fig. 3b. Based on the relative stability of Mn^{4+}, Mn^{3+} and Mn^{2+} cations [31,32] this is unlikely.

Therefore an alternative model is proposed in which it is assumed that no charge disproportionation takes place by the defect reaction (3) but that neutral $\langle Mn'-V_O^{\cdot\cdot}-Mn' \rangle$ clusters are formed at low oxygen partial pressures by the following defect reaction:

$$2Mn_{Mn}^{\times} + O_O^{\times} \rightleftarrows \langle Mn_{Mn}'-V_O^{\cdot\cdot}-Mn_{Mn}' \rangle + \tfrac{1}{2}O_2 , \quad (11)$$

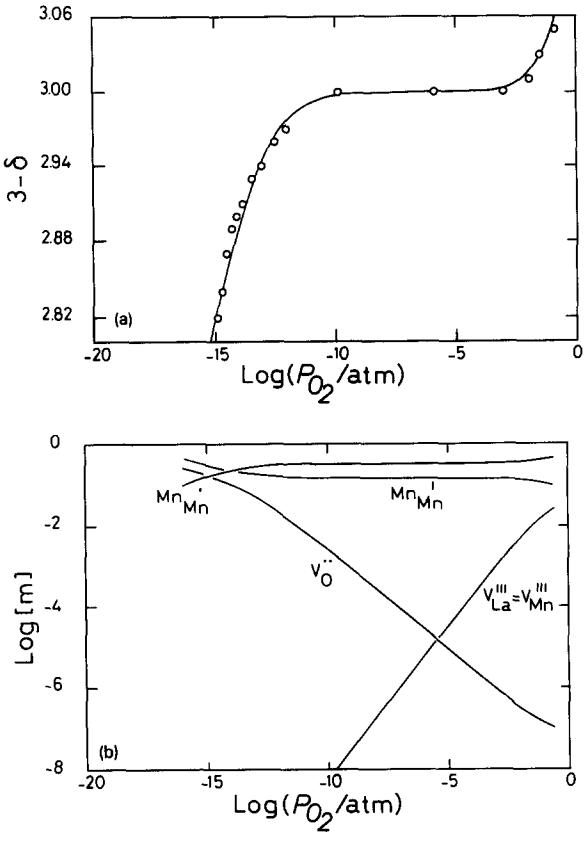

Fig. 3. (a) A comparison between the experimentally determined [15] (open circle) and the calculated nonstoichiometry (drawn line) of $La_{0.8}Sr_{0.2}MnO_3$ at 1000°C using the defect reactions (2), (3) and (9). The model parameters are shown in table 2 ($La_{1-y}Sr_yMnO_3$ "excess"); (b) the defect mole fractions corresponding to the nonstoichiometry isotherm of (a).

Table 2
Model parameters for the calculation of the nonstoichiometry of $La_{1-y}Sr_yMnO_3$ at 1000°C.

Parameter	$La_{1-y}Sr_yMnO_3$ "excess"	$La_{1-y}Sr_yMnO_3$ "excess+cluster"
y	0.2	0.2
K_2 ($atm^{1/2}$)	4×10^{-8}	3×10^{-7}
K_3	9.5×10^{-2}	
K_9 ($atm^{-3/2}$)	10^{-2}	6×10^{-4}
K_{11} ($atm^{1/2}$)		1.67×10^{-9}

with the equilibrium constant:

$$K_{11} = \frac{[\langle Mn'_{Mn} - V_O^{\cdot\cdot} - Mn'_{Mn} \rangle] P_{O_2}^{1/2}}{[Mn_{Mn}^{\times}]^2 [O_O^{\times}]} . \quad (12)$$

The defect reaction (11) was proposed for the first time by Roosmalen et al. [19] to describe the nonstoichiometry of $LaMnO_3$. As shown here, the same defect reaction can be used to model the nonstoichiometry of $La_{1-y}Sr_yMnO_3$. Eq. (7), with replacement of Fe by Mn, should still be fulfilled and the charge neutrality condition demands that:

$$[Sr'_{La}] + 3[V'''_{La}] + 3[V'''_{Mn}] = [Mn^{\cdot}_{Mn}] + 2[V_O^{\cdot\cdot}] . \quad (13)$$

The model parameters for this "defect cluster and oxygen excess" model are shown in table 2 ($La_{1-y}Sr_yMnO_3$ "excess+cluster"). Fig. 4a shows that a good fit is obtained with the experimental data of the nonstoichiometry of $La_{0.8}Sr_{0.2}MnO_3$, whereas fig. 4b shows that according to the model description part of the oxygen vacancies is randomly distributed over the available sites and all the other oxygen vacancies are bound in the neutral $\langle Mn' - V_O^{\cdot\cdot} - Mn' \rangle$ clusters.

However, no analytical expression was obtained for the oxygen permeation current density on the basis of the "defect cluster and oxygen excess" model. Therefore the random point defect model developed for $La_{1-y}Sr_yCrO_3$, $La_{1-y}Sr_yFeO_3$ and $La_{1-y}Sr_yCoO_3$ is also used as an approximation to compute the oxygen permeation current density through $La_{0.8}Sr_{0.2}MnO_3$.

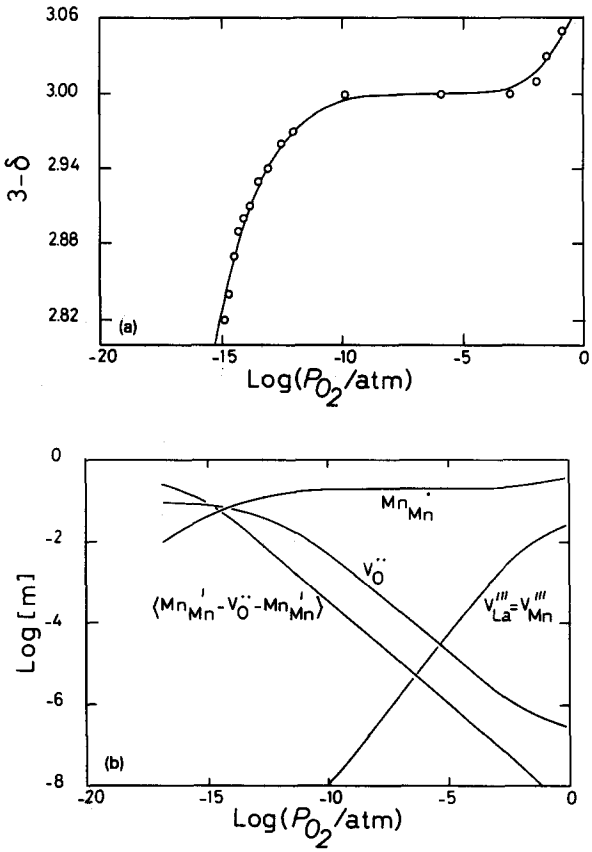

Fig. 4. (a) A comparison between the experimentally determined ref. [15] (open circle) and the calculated nonstoichiometry (drawn line) of $La_{0.8}Sr_{0.2}MnO_3$ at 1000°C using the defect reactions (2), (9) and (11). The model parameters are shown in table 2 ($La_{1-y}Sr_yMnO_3$ "excess+cluster"); (b) the defect mole fractions corresponding to the nonstoichiometry isotherm of (a).

2.2. Oxygen permeation

In the following analysis, a mixed conducting oxide is considered in which oxygen ions and electrons or corresponding lattice defects are mobile. When such a material is placed in an oxygen potential gradient, oxygen ions will move through the membrane from the high to the low oxygen partial pressure side (fig. 5). The electrons will migrate in the opposite direction. The driving force for the chemical diffusion is the gradient of the chemical potential of oxygen.

When the electronic conductivity is much higher than the ionic conductivity (the electronic transference number can be approximated as unity), the ox-

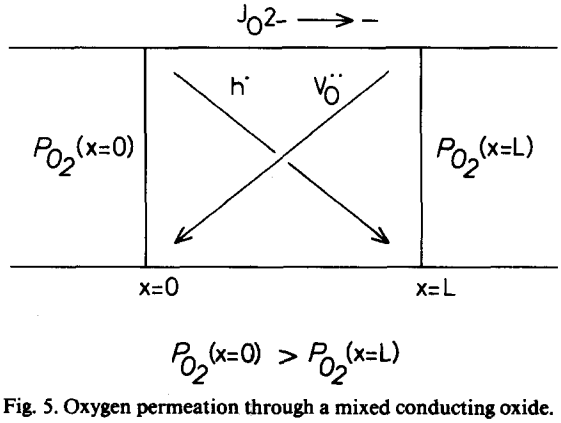

Fig. 5. Oxygen permeation through a mixed conducting oxide.

ygen permeation current density can be calculated from the following equation [10,20,21]:

$$J_{O^{2-}}(\mathrm{Am}^{-2}) = -\frac{1}{L}\int_{P_{O_2}(x=0)}^{P_{O_2}(x=L)} \sigma_{O^{2-}}\frac{RT}{4F}\,\mathrm{d}\ln P_{O_2}. \qquad (14)$$

In the derivation of this equation, it has been assumed that the fluxes of the oxygen ions and electrons or holes are related to each other by the condition of charge neutrality and that local equilibrium of the defect reactions prevails. In the transport equations, the non-ideality or cross terms for the fluxes of ions and electrons are neglected [7,10].

When all oxygen vacancies are fully ionized and contribute to the ionic conductivity of the $ABO_{3-\delta}$ perovskite, the ionic conductivity can be calculated from

$$\sigma_{O^{2-}}(\Omega^{-1}\,\mathrm{m}^{-1}) = \frac{4F^2[V_O^{\cdot\cdot}]D_V}{RTV_m}, \qquad (15)$$

where R is the molar gas constant (J mol^{-1} K^{-1}), T, the absolute temperature (K), $[V_O^{\cdot\cdot}]$, the oxygen vacancy mole fraction, D_V, the vacancy diffusion coefficient (m^2 s^{-1}) and V_m is the molar volume of perovskite (m^3 mol^{-1}).

The substitution of eqs. (8) and (15) into eq. (14) results in the following integral equation:

$$\begin{aligned} J_{O^{2-}}(\mathrm{Am}^{-2}) = -\frac{2FD_V}{LV_m} \times \Bigg(& \int_{[Fe_{Fe}^{\cdot}(x=0)]}^{[Fe_{Fe}^{\cdot}(x=L)]} [V_O^{\cdot\cdot}]\,\mathrm{d}\ln[Fe_{Fe}^{\cdot}] \\ & + \int_{[O_O^{\times}(x=0)]}^{[O_O^{\times}(x=L)]} [V_O^{\cdot\cdot}]\,\mathrm{d}\ln[O_O^{\times}] \\ & - \int_{[Fe'_{Fe}(x=0)]}^{[Fe'_{Fe}(x=L)]} [V_O^{\cdot\cdot}]\,\mathrm{d}\ln[Fe'_{Fe}] \\ & - \int_{[V_O^{\cdot\cdot}(x=0)]}^{[V_O^{\cdot\cdot}(x=L)]} [V_O^{\cdot\cdot}]\,\mathrm{d}\ln[V_O^{\cdot\cdot}] \Bigg). \end{aligned} \qquad (16)$$

The molar volume of the perovskite and the vacancy diffusion coefficient are assumed to be independent of the nonstoichiometry. The oxygen vacancy mole fraction $[V_O^{\cdot\cdot}]$ can be expressed as a function of $[F'_{Fe}]$ or $[Fe_{Fe}^{\cdot}]$ by using the eqs. (4)–(7). In this way it is possible to solve the integral equation, the final result being shown in Appendix A.1.

The oxygen permeation current density through 1 mm thick layers of the $La_{0.75}Sr_{0.25}CrO_3$, $La_{0.9}Sr_{0.1}FeO_3$, $La_{0.9}Sr_{0.1}CoO_3$ and $La_{0.8}Sr_{0.2}MnO_3$ perovskites has been calculated as a function of the oxygen partial pressure gradient by using the model parameters of table 1 and is shown in fig. 6. When the oxygen partial pressure at the high oxygen partial pressure side ($x=0$) is 1 atm, then the oxygen permeation current density of $La_{0.75}Sr_{0.25}CrO_3$,

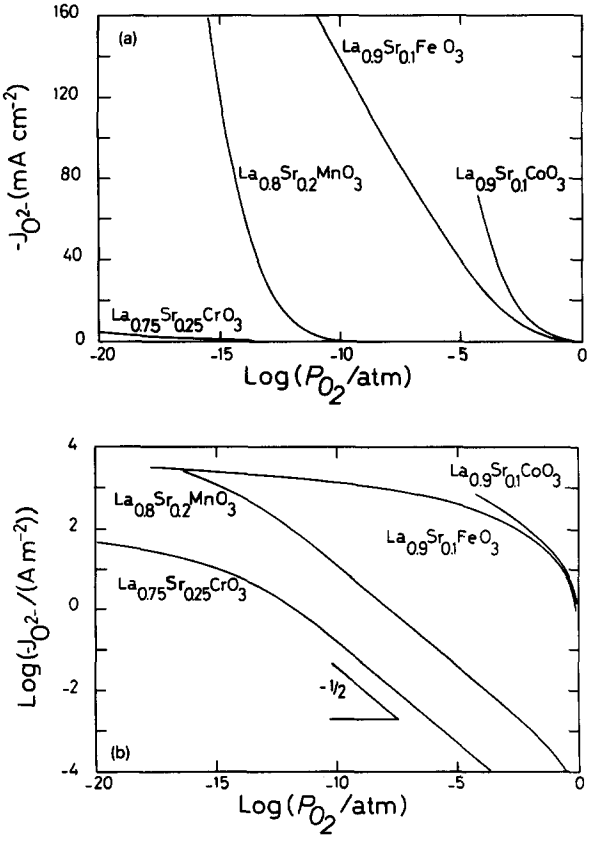

Fig. 6. (a) The oxygen permeation current density through 1 mm thick layers of $La_{0.75}Sr_{0.25}CrO_3$, $La_{0.9}Sr_{0.1}FeO_3$, $La_{0.9}Sr_{0.1}CoO_3$ and $La_{0.8}Sr_{0.2}MnO_3$ at 1000°C as a function of the oxygen partial pressure at the low oxygen partial pressure side ($P_{O_2}(x=0)=1$ atm). $J_{O^{2-}}$ was calculated from eq. (16) using the model parameters of table 1; (b) the logarithm of the oxygen permeation current density as shown in (a).

$La_{0.8}Sr_{0.2}MnO_3$ and $La_{0.9}Sr_{0.1}CoO_3$ depends on the oxygen partial pressure at the low oxygen partial pressure side ($x=L$) as $J_{O^{2-}} \propto P_{O_2}^{-1/2}$. For $La_{0.9}Sr_{0.1}FeO_3$, this dependence is different and given by $J_{O^{2-}} \propto \log(P_{O_2})$. A possible explanation for the P_{O_2} dependence of $J_{O^{2-}}$ will be given later.

The oxygen permeation current density of $La_{0.75}Sr_{0.25}CrO_3$ and $La_{0.8}Sr_{0.2}MnO_3$ does not depend on the oxygen partial pressure at the high oxygen partial pressure side when the nonstoichiometry at the low oxygen partial pressure side is high. This results from the fact that $[V_O^{\cdot\cdot}(x=0)]$ is very small in comparison with $[V_O^{\cdot\cdot}(x=L)]$ even when the $P_{O_2}(x=0)$ is changed over some decades. In the case of $La_{0.9}Sr_{0.1}FeO_3$ and $La_{0.9}Sr_{0.1}CoO_3$ their nonstoichiometry can be considerable at the high oxygen partial pressure side which makes the oxygen permeation current density also dependent on the oxygen partial pressure at that side.

2.3. Limiting surface oxygen exchange rate

Upon reducing the membrane thickness, the oxygen permeation may become controlled by a limiting surface oxygen exchange rate [10,22,23]. The gradient in the oxygen chemical potential will be largely consumed by the surface exchange kinetics at the expense of the gradient across the oxide bulk. The following boundary condition can be used to model the effect of a limiting surface oxygen exchange process:

$$J_{O^{2-}}(\mathrm{Am^{-2}}) = \frac{2Fk_s'}{V_m}\left([V_O^{\cdot\cdot}]_s' - [V_O^{\cdot\cdot}]_{eq}'\right) \quad \text{at } x=0, \tag{17}$$

$$J_{O^{2-}}(\mathrm{Am^{-2}}) = \frac{2Fk_s''}{V_m}\left([V_O^{\cdot\cdot}]_{eq}'' - [V_O^{\cdot\cdot}]_s''\right) \quad \text{at } x=L, \tag{18}$$

where $[V_O^{\cdot\cdot}]_s$ is the oxygen vacancy mole fraction at the surface when $J_{O^{2-}} \neq 0$. $[V_O^{\cdot\cdot}]_{eq}$ is the oxygen vacancy mole fraction when in equilibrium with the gas phase ($J_{O^{2-}}=0$), and k_s is the surface oxygen exchange rate constant ($\mathrm{m\,s^{-1}}$).

The surface oxygen exchange rate constant can take different values at both sides of the perovskite membrane. Depending on the values of the rate constants, the oxygen permeation can become limited by the oxygen exchange at the high oxygen partial pressure side, by the diffusion inside the perovskite or by the oxygen exchange at the low oxygen partial pressure side. The rate constants may depend on the oxygen partial pressure in the gas phase [2]. For the sake of illustration, the oxygen permeability of $La_{0.9}Sr_{0.1}FeO_3$ was calculated assuming surface exchange rate limitation at the high oxygen partial pressure side. In fig. 7, it is shown how different values of the oxygen exchange rate at that side affect the oxygen partial pressure dependence of the oxygen permeation current density through a 1 mm thick layer of $La_{0.9}Sr_{0.1}FeO_3$.

Surface oxygen exchange rate constants can be determined with the ^{18}O isotope exchange technique [16,17]. Those rate constants are, however, obtained when the material is in equilibrium with the gas phase. So there is no change of the nonstoichiometry during the experiment. Some data about the ^{18}O isotope exchange rate are collected in table 3.

Data on the non-equilibrium kinetics of oxygen exchange can be obtained by weight change experiments as a function of time after a sudden change of the oxygen partial pressure or a similar experiment by measuring the conductivity [2]. As in this kind of experiments reactive gases are used like CO/CO_2 or H_2/H_2O mixtures, the surface exchange kinetics

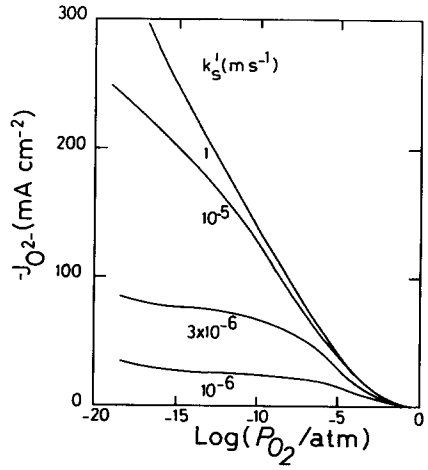

Fig. 7. The effect of a limiting surface oxygen exchange rate at the high oxygen partial pressure side on the oxygen permeation current density of $La_{0.9}Sr_{0.1}FeO_3$ ($k_s''=1\ \mathrm{m\,s^{-1}}$, $L=1$ mm).

Table 3
Literature values of the surface oxygen exchange rate.

Perovskite	Temp. (K)	P_{O_2} (atm)	V_m ($m^3\,mol^{-1}$)	k_s ($cm\,s^{-1}$)	Method
$La_{0.9}Sr_{0.1}CoO_3$	1273	4.5×10^{-2}	3.4×10^{-5}	2.31×10^{-6}	^{18}O isotope exchange [17]
$La_{0.9}Sr_{0.1}FeO_3$	1273	6.5×10^{-2}	3.62×10^{-5}	1.85×10^{-6}	^{18}O isotope exchange [17]
$La_{0.8}Sr_{0.2}MnO_3$	1173	0.75	3.56×10^{-5}	5×10^{-8}	^{18}O isotope exchange [16]
$La_{0.7}Ca_{0.3}CrO_3$	1273	10^{-15}	3.38×10^{-5}	3.2×10^{-4}	conductivity relaxation [2]

may differ from the ^{18}O isotope exchange process.

3. Discussion

The point defect model presented in section 2.1 is useful for modelling the nonstoichiometry of the $A_{1-y}A'_yBO_3$ (A=La, Y; A′=Ca, Sr; B=Cr, Fe, Co, Mn) perovskites at temperatures and oxygen partial pressures where they show the stable single phase perovskite structure. Some perovskites, however, show a nearly stoichiometric composition at high oxygen partial pressures. The oxygen nonstoichiometry calculated from the point defect can then be verified only at low oxygen partial pressures where the nonstoichiometry is measurable by thermogravimetric measurements or coulometric titration. The oxygen vacancy concentration at high oxygen partial pressures is too small to be measured by those techniques. It is, however, assumed that the oxygen vacancy concentration at high oxygen partial pressures can also be calculated with the same point defect model but this needs further experimental verification.

In the point defect model, the oxygen vacancies are assumed to be fully ionized. This seems reasonable at high temperatures but at lower temperatures differently charged oxygen vacancies may be present: $\delta=[V_O^{\cdot\cdot}]+[V_O^{\cdot}]+[V_O^{\times}]$.

Deviations from the point defect model might also occur at high defect concentrations. Due to interactions between the defects, extended point defects may form. For instance a neutral $\langle Mn'-V_O^{\cdot\cdot}-Mn'\rangle$ cluster may be formed in $La_{0.8}Sr_{0.2}MnO_3$ at low oxygen partial pressures. When the nonstoichiometry is high, the oxygen vacancies may also order. Then they no longer contribute to diffusion and conductivity. Numerous examples of vacancy ordering in $ABO_{3-\delta}$ oxides have been discussed by Rao and Gopalakrishnan [24]. In addition, the vacancy diffusion coefficient can no longer be treated as independent of the oxygen vacancy mole fraction when the nonstoichiometry is high.

The presence of differently charged oxygen vacancies and maybe oxygen vacancies in a cluster like $\langle Mn'-V_O^{\cdot\cdot}-Mn'\rangle$ will result in a complicated expression for the chemical diffusion coefficient of oxygen. The diffusion of oxygen in a mixed conductor with many different types of ionic species and with oxygen vacancies with a variable ionization degree has been discussed by Liu [10] and Maier [25]. From these considerations, it was decided to limit the model calculation of the oxygen permeation current density to small dopant mole fractions and a relatively high temperature.

Perovskites like $La_{0.75}Sr_{0.25}CrO_3$ and $La_{0.8}Sr_{0.2}MnO_3$ show a very small oxygen permeation current density in an oxygen partial pressure gradient of 1 atm to 10^{-4} atm. They will show an increase of the oxygen permeation current density when the oxygen partial pressure at the low oxygen partial pressure side is further decreased. This results from an increase of their nonstoichiometry. This may be overlooked in experimental studies which rely on a gaschromatographic analysis of the oxygen permeation rate. In that kind of studies, He gas is used with a constant oxygen partial pressure of about 10^{-4} atm at the low oxygen partial pressure side of the membrane. The oxygen partial pressure at the low oxygen partial pressure side could be varied by using

CO/CO_2 or H_2/H_2O mixtures. An analysis of all the products which are formed by the reaction with the permeating oxygen will make it possible to determine the oxygen permeation current density. Changing the gas composition from He to CO/CO_2 or H_2/H_2O mixtures may effect the surface exchange kinetics. An electrochemical cell for the measurement of the oxygen permeation current density in a large oxygen partial pressure gradient was proposed by Sakai et al. [26].

From an experimental point of view, it is important to know how the oxygen permeation current density depends on the oxygen partial pressure gradient and the membrane thickness. According to eq. (16), the oxygen permeation current density is inversely proportional to the membrane thickness when the oxygen permeation is rate determined by the diffusion inside the perovskite. It results in a parabolic rate law for the growth of perovskite layers by the EVD method [27]. The oxygen permeation becomes independent of the membrane thickness when limited exclusively by the surface oxygen exchange process.

The oxygen partial pressure dependence of the oxygen permeation current density reflects the nonstoichiometry when the oxygen permeation current density is rate determined by diffusion inside the perovskite. From the slope of the oxygen permeation current density versus the logarithm of the oxygen partial pressure, the oxygen vacancy mole fraction can be calculated. Using eq. (15) into eq. (14) and differentiation with respect to the $\ln P_{O_2}(x=L)$ gives:

$$\left(\frac{dJ_{O^{2-}}}{d\ln P_{O_2}}\right) = -\frac{F[V_O^{\cdot\cdot}]D_V}{LV_m}. \qquad (19)$$

A constant oxygen vacancy mole fraction will result in the following relation between the oxygen permeation current density and the oxygen partial pressure gradient:

$$J_{O^{2-}}(Am^{-2}) = \frac{F[V_O^{\cdot\cdot}]D_V}{LV_m}\ln\left(\frac{P_{O_2}(x=0)}{P_{O_2}(x=L)}\right). \qquad (20)$$

$La_{0.9}Sr_{0.1}FeO_3$ is one of the perovskites which shows such a logarithmic dependence on the oxygen partial pressure (fig. 6a). This results from the fact that its nonstoichiometry takes a constant value $[V_O^{\cdot\cdot}] = y/2$ in a broad range of the oxygen partial pressure. The oxygen permeation current density of the $La_{0.75}Sr_{0.25}CrO_3$, $La_{0.8}Sr_{0.2}MnO_3$ and $La_{0.9}Sr_{0.1}CoO_3$ perovskites depends on the oxygen partial pressure at the low oxygen partial pressure side according to $J_{O^{2-}} \propto P_{O_2}^{-1/2}$ (fig. 6b). This is the same as the oxygen partial pressure dependence of the oxygen vacancy mole fraction (fig. 2).

Some perovskites cannot be used as a membrane in a large oxygen partial pressure gradient. For instance, $La_{0.9}Sr_{0.1}CoO_3$ decomposes if exposed at oxygen partial pressures lower than 10^{-4} atm at 1000°C [14]. It could be considered to protect the perovskite against decomposition by applying a thin layer of a more stable perovskite at the low oxygen partial pressure side. The result is a ceramic membrane which is stable in a large oxygen partial pressure gradient.

4. Conclusion

In modelling the oxygen permeation of the $La_{0.75}Sr_{0.25}CrO_3$, $La_{0.9}Sr_{0.1}FeO_3$, $La_{0.9}Sr_{0.1}CoO_3$ and $La_{0.8}Sr_{0.2}MnO_3$ perovskites it is important to consider the oxygen partial pressure dependence of the ionic conductivity. As a first approximation this can be calculated using a point defect model.

Accurate predictions of the oxygen permeation current density are possible only when the nonstoichiometry is known in the oxygen partial pressure gradient under study. Model parameters can then be obtained by fitting the point defect model to the experimentally determined nonstoichiometry.

When the membrane is very thin or when the membrane is placed in a large oxygen potential gradient, then the surface oxygen exchange process will partially limit the oxygen permeation current density. As a first approximation, a linear boundary condition can be used to model such rate limitation of the oxygen permeation current density.

Acknowledgement

This work was performed as a R&D program of the Moonlight Project of the Agency of Industrial Science and Technology of Japan (Ministry of International Trade and Industry). The support of the

Science and Technology Agency of Japan is greatly acknowledged.

Appendix A.1. Integration by parts of the oxygen permeation current density integral equation

When the $[Fe_{Fe}^{\cdot}]$ and $[Fe_{Fe}']$ mole fractions are abbreviated as a and b, respectively, then the integration of eq. (16) by parts results in:

$$\int_{[O_O^{\times}(x=0)]}^{[O_O^{\times}(x=L)]} [V_O^{\cdot\cdot}]\,d\ln[O_O^{\times}] - \int_{[V_O^{\cdot\cdot}(x=0)]}^{[V_O^{\cdot\cdot}(x=L)]} [V_O^{\cdot\cdot}]\,d\ln[V_O^{\cdot\cdot}] = [3\ln(3-[V_O^{\cdot\cdot}])]_{[V_O^{\cdot\cdot}(x=0)]}^{[V_O^{\cdot\cdot}(x=L)]}, \tag{21}$$

$$\int_{b(x=0)}^{b(x=L)} [V_O^{\cdot\cdot}]\,d\ln b = \left[-\frac{(1-y)}{2}\ln b + \frac{(4K_3-1)b}{4K_3} + \frac{\sqrt{b^2(1-4K_3)+4bK_3}}{4K_3} + \frac{1}{2\sqrt{1-4K_3}}\ln\left(2\sqrt{(1-4K_3)(b^2(1-4K_3)+4bK_3)}+2(1-4K_3)b+4K_3\right)\right]_{b(x=0)}^{b(x=L)}, \tag{22}$$

$$\int_{a(x=0)}^{a(x=L)} [V_O^{\cdot\cdot}]\,d\ln a = \left[+\frac{(1+y)}{2}\ln a + \frac{(1-4K_3)a}{4K_3} - \frac{\sqrt{a^2(1-4K_3)+4aK_3}}{4K_3} - \frac{1}{2\sqrt{1-4K_3}}\ln\left(2\sqrt{(1-4K_3)(a^2(1-4K_3)+4aK_3)}+2(1-4K_3)a+4K_3\right)\right]_{a(x=0)}^{a(x=L)}. \tag{23}$$

The oxygen permeation current density can be obtained from eq. (16) by substitution of the mole fractions of the defects at the high ($x=0$) and low ($x=L$) oxygen partial pressure side of the perovskite membrane.

References

[1] N. Sakai, T. Kawada, H. Yokokawa and M. Dokiya, Proc. Second Intern. Symp. Solid Oxide Fuel Cells, Athens, Greece, 2–5 July 1991, eds. F. Grosz, P. Zegers, S.C. Singhal and O. Yamamoto (Comm. Europ. Commun. Report EUR13546 EN) pp. 629–636.

[2] I. Yasuda and T. Hikita, Proc. Second Intern. Symp. Solid Oxide Fuel Cells, Athens, Greece, 2–5 July 1991, eds. F. Grosz, P. Zegers, S.C. Singhal and O. Yamamoto (Comm. Europ. Commun. Report EUR13546 EN) pp. 645–652.

[3] B.A. van Hassel, T. Kawada, N. Sakai, H. Yokokawa and M. Dokiya, Solid State Ionics 66 (1993) 41.

[4] O. Yamamoto, Y. Takeda, R. Kanno and M. Noda, Solid State Ionics 22 (1987) 241.

[5] Y. Teraoka, T. Nobunaga, K. Okamoto, N. Miura and N. Yamazoe, Solid State Ionics 48 (1991) 207.

[6] A.J. Burggraaf, H.J.M. Bouwmeester, B.A. Boukamp, R.J.R. Uhlhorn and V. Zaspalis, in: Science of Ceramic Interfaces, ed. J. Nowotny (Elsevier Amsterdam, 1991) pp. 525–568.

[7] C. Wagner, Prog. Solid State Chem. 10 (1975) 3.

[8] H.-H. Möbius, Z. Chem., to be published.

[9] T.A. Ramanarayanan, S. Ling and M.P. Anderson, Proc. Second Intern. Symp. Solid Oxide Fuel Cells, Athens, Greece, 2–5 July 1991, eds. F. Grosz, P. Zegers, S.C. Singhal and O. Yamamoto (Comm. Europ. Commun. Report EUR13546 EN) pp. 777–786.

[10] M. Liu, Proc. First Intern. Symp. Ionic and Mixed Conducting Ceramics, 180th Meeting of the Electrochem. Soc. in Phoenix, Arizona, October 16–17, 1991, Proc. Vol. 91–12, eds. T.A. Ramanarayanan and H.L. Tuller, pp. 191–215.

[11] J. Mizusaki, S. Yamauchi, K. Fueki and A. Ishikawa, Solid State Ionics 12 (1984) 119.

[12] G.F. Carini, H.U. Anderson, D.M. Sparlin and M.M. Nasrallah, Solid State Ionics 49 (1991) 233.

[13] J. Mizusaki, M. Yoshihiro, S. Yamauchi and K. Fueki, J. Solid State Chem. 58 (1985) 257.

[14] J. Mizusaki, Y. Mima, S. Yamauchi, K. Fueki and H. Tagawa, J. Solid State Chem. 80 (1989) 102.

[15] J.H. Kuo, H.U. Anderson and D.M. Sparlin, J. Solid State Chem. 83 (1989) 52.
[16] S. Carter, A. Selcuk, R.J. Chater, J. Kajda, J.A. Kilner and B.C.H. Steele, Solid State Ionics 53–56 (1992) 597.
[17] T. Ishigaki, S. Yamauchi, K. Kishio, J. Mizusaki and K. Fueki, J. Solid State Chem. 73 (1988) 179.
[18] F.A. Kröger and H.J. Vink, in: Solid State Physics, eds. F. Seitz and P. Turnbull, Vol. 3 (Academic Press, New York, 1956).
[19] J.A.M. van Roosmalen and E.H.P. Cordfunke, J. Solid State Chem. 93 (1991) 212.
[20] G.J. Dudley and B.C.H. Steele, J. Solid State Chem. 31 (1980) 233.
[21] W. Weppner and R.A. Huggins, Ann. Rev. Mat. Sci. 8 (1978) 269.
[22] S. Dou, C.R. Mason and P.D. Pacey, J. Electrochem. Soc. 132 (1985) 1843.
[23] H.J.M. Bouwmeester, H. Kruidhof, A.J. Burggraaf and P.J. Gellings, Solid State Ionics 53–56 (1992) 460.
[24] C.N.R. Rao and J. Gopalakrishnan, New Directions in Solid State Chemistry: Structure, Synthesis, Properties, Reactivity and Materials Design, Cambridge Solid State Science Series, eds. R.W. Cahn, E.A. Davis and I.M. Ward (Cambridge University Press, Cambridge, 1986) pp. 208–263.
[25] J. Maier, Solid State Ionics 57 (1992) 71.
[26] N. Sakai, T. Horita, B.A. van Hassel, T. Kawada, H. Yokokawa and M. Dokiya, Proc. 18th Symp. Solid State Ionics in Japan, October 12–13, 1992, Fukuoka (The Solid State Ionics Society of Japan, Tokyo, 1992) p. 93.
[27] J. Schoonman, J.P. Dekker, J.W. Broers and N.J. Kiwiet, Solid State Ionics 46 (1991) 299.
[28] Y. Yamamura, Y. Ninomiya and S. Sekido, Proc. Intern. Meeting on Chemical Sensors, ed. T. Seiyama (Elsevier, Amsterdam, 1983) pp. 187–192.
[29] Powder Diffraction File, JCPDS – International Centre for Diffraction Data, no. 28–1229, 32–1240, 35–1480 and 40–1100.
[30] B.C.H. Steele, S. Carter, J. Kajda, I. Kontoulis and J.A. Kilner, Proc. Second Intern. Symp. on Solid Oxide Fuel Cells, Athens, Greece, 2–5 July 1991, eds. F. Grosz, P. Zegers, S.C. Singhal and O. Yamamoto (Comm. Europ. Commun. Report EUR13546 EN) pp. 517–525.
[31] H. Yokokawa, N. Sakai, T. Kawada and M. Dokiya, Proc. Intern. Symp. Solid Oxide Fuel Cells, Nagoya, Japan, November 13–14, 1989 (Science House, Tokyo, 1990) pp. 118–134.
[32] H. Yokokawa, N. Sakai, T. Kawada and M. Dokiya, Proc. 5th Internat. Conf. on Science and Technology of Zirconia (Technomic Publ. Co., Inc., Lancaster, PA, 1993), to be published.